



# Printed environmentally friendly supercapacitors with ionic liquid electrolytes on paper

F. Pettersson<sup>a,\*</sup>, J. Keskinen<sup>b</sup>, T. Remonen<sup>a,c</sup>, L. von Hertzen<sup>d</sup>, E. Jansson<sup>e</sup>, K. Tappura<sup>b</sup>, Y. Zhang<sup>c</sup>, C.-E. Wilén<sup>c</sup>, R. Österbacka<sup>a</sup>

<sup>a</sup> Department of Natural Sciences/Physics, Åbo Akademi University, Porthaninkatu 3, FI-20500 Turku, Finland

<sup>b</sup> VTT Technical Research Centre of Finland, Sinitaival 6, PO Box 1300, FI-33101 Tampere, Finland

<sup>c</sup> Department of Chemical Engineering/Polymer Technology, Åbo Akademi University, Piispankatu 8, FI-20500 Turku, Finland

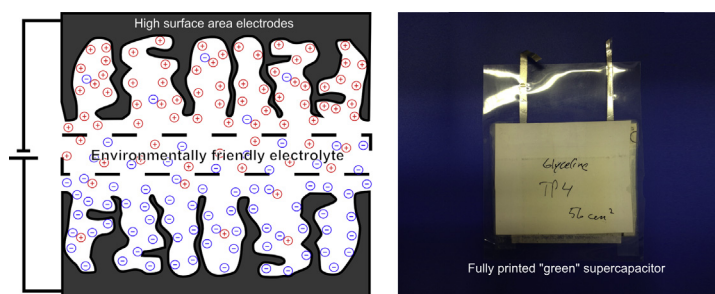
<sup>d</sup> VTT Technical Research Centre of Finland, Biologinkuja 7, PO Box 1000, FI-02044 Espoo, Finland

<sup>e</sup> VTT Technical Research Centre of Finland, Kaitoväylä 1, PO Box 1100, FI-90571 Oulu, Finland

## HIGHLIGHTS

- Environmentally friendly supercapacitors are fabricated on a paper substrate.
- Deep eutectic solvents based on chlorine chloride are used as electrolyte.
- The materials used are inexpensive and the entire supercapacitor is printed.
- Electrodes are printed using a screen printer in a pilot scale production line.
- Glyceline™ has the highest capacitance and highest power density.

## GRAPHICAL ABSTRACT



## ARTICLE INFO

### Article history:

Received 21 March 2014

Received in revised form

17 July 2014

Accepted 4 August 2014

Available online 12 August 2014

### Keywords:

Supercapacitor

Deep eutectic solvent

Printed

Environmentally friendly

Activated carbon

## ABSTRACT

Environmentally friendly supercapacitors are fabricated using commercial grade aluminum coated paper as a substrate and symmetrical activated carbon electrodes as large area electrodes. Different choline chloride-based eutectic solvents are used as electrolyte. These are inexpensive, environmentally friendly and have a larger operating window compared to that of water electrolytes. As the entire device is printed and the materials used are inexpensive, both small- and large-area power sources can be fabricated to be used in cheap, disposable and recyclable devices. Supercapacitors with different eutectic solvents are measured using cyclic charge–discharge and impedance spectroscopy measurements and compared to one widely used and one “green” imidazolium ionic liquid; EMIM:TFSI and EcoEng 212™, respectively. A mixture of ethylene glycol and choline chloride, Glyceline™, show the highest capacitance and power densities of the electrolytes being tested, including the imidazolium alternatives.

© 2014 Elsevier B.V. All rights reserved.

\* Corresponding author. Tel.: +358 40 7428689.

E-mail addresses: [Fredrik.Pettersson@abo.fi](mailto:Fredrik.Pettersson@abo.fi) (F. Pettersson), [Jari.Keskinen@vtt.fi](mailto:Jari.Keskinen@vtt.fi) (J. Keskinen), [Tommie.Remonen@abo.fi](mailto:Tommie.Remonen@abo.fi) (T. Remonen), [Leo.vonHertzen@vtt.fi](mailto:Leo.vonHertzen@vtt.fi) (L. von Hertzen), [Elina.Jansson@vtt.fi](mailto:Elina.Jansson@vtt.fi) (E. Jansson), [Kirsi.Tappura@vtt.fi](mailto:Kirsi.Tappura@vtt.fi) (K. Tappura), [Yanxi.Zhang@rug.nl](mailto:Yanxi.Zhang@rug.nl) (Y. Zhang), [Carl-Erik.Wilen@abo.fi](mailto:Carl-Erik.Wilen@abo.fi) (C.-E. Wilén), [Ronald.Osterbacka@abo.fi](mailto:Ronald.Osterbacka@abo.fi) (R. Österbacka).

## 1. Introduction

Supercapacitors (SC) [1] are used in energy storage applications especially when high power peaks are required to be absorbed (stored) or delivered. A typical SC consists of two large area

electrodes separated by a porous membrane, i.e. a separator. The electrodes are typically made of activated carbon (AC) powder that is bound using fluorine containing polymers. The ion conductive electrolyte fills the voids in the electrodes and the separator. As electrolytes, aqueous alternatives containing e.g. KOH [2], H<sub>2</sub>SO<sub>4</sub> [2], and even NaCl or other salts such as sulfates and carbonates are often used [3]. But also organic solutions such as propylene carbonate or acetonitrile with tetraalkylammonium salts [4–6] or ionic liquids (IL) [7–9] such as EMIM:TFSI [10] are also commonly used. In high power density applications, or when making small SCs, the organic alternatives are advantageous as they can withstand voltages up to 3–5 V (water electrolyte SC degrade around 1.2–1.5 V) giving higher power densities and, hence, higher powers per unit area are reached.

Today's society is increasingly moving towards capturing and transmitting data, i.e. moving towards realizing “the Internet of Things”, where everything is connected. To reach this there is a need for small sized power sources that can be applied in identification and data storage/transfer devices as well as in miniaturized sensors systems. The supercapacitor being a simple power device, both in terms of materials choices as well as in fabrication processes, can be of great use in such applications. Active type tags and sensors require a suitable power source to fully utilize their potential allowing greater memory capacity in the tag and increasing the range from which the tag can be read [11]. These tags are often intended to be used as integrated parts of recyclable or disposable (burnable or biodegradable) products. Hence the materials of choice should be inexpensive and safe, and obviously the manufacturing methods and materials choice should both result in low-cost products as well as having a low carbon footprint. Further, many of the objects/things envisaged of being tagged are by themselves small, or the tag needs to be nonintrusive (or physically small for other reasons). Here, a solution which combines the environmental friendliness of water electrolytes with the higher voltage capabilities (i.e. higher power per unit area) of the organic salts (IL and/or organic salt solutions) would be attractive. These demands are not easily met using the traditional materials and material combinations mentioned above.

In the above described applications photovoltaic cells or small size primary or secondary batteries can be used as the main power source. On the other hand a combination of any of these with a SC is also a feasible possibility, especially for applications where high current output is required only for short periods of time. For instance environmentally friendly biobatteries – although providing low peak current output on their own – is a “green” alternative that can be used in a wide range of applications when integrated with a printed supercapacitor [12].

The manufacturing of these small sized supercapacitors by printing methods is essential to facilitate inexpensive manufacturing process. The same manufacturing route can be applied when preparing supercapacitors of larger sizes and/or for other applications, as printing processes allow up-scaling by facilitating the manufacturing of either a large number of small components or large area ones. The manufacturing of supercapacitor electrodes using printing techniques has been described in patents [13,14] and scientific reports [12,15–21]. A solution based process that can be modified to screen printing has been reported in the preparation of polyaniline-based supercapacitors [22]. Batteries and supercapacitors of carbon nanotubes and room-temperature ionic liquid electrolytes have been constructed using paper as a substrate material [23].

The supercapacitors presented in this paper are of the non-Faradaic electric double layer capacitor (EDLC) kind. This means that no charge is transferring between the electrode and the ion conductive dielectric when the capacitor is being charged i.e. the

charge is being stored electrostatically on the electrodes. As there are no electrochemical processes (ideally) taking place, i.e. no reduction or oxidation of/at the electrodes, the supercapacitors can stand more charging- and discharging cycles (>100,000 switches) than secondary batteries, in which reduction/oxidation processes typically reduce the cycle life to below 5000 cycles.

Environmentally friendly SC have previously been realized using water-based electrolytes with NaCl as the salt. [17] These devices, however, are limited by their operating window as water is electrochemically dissociated above 1.23 V. This severely limits their power storage capabilities and to achieve higher voltages the SC cells need to be serially connected which complicates their manufacturing processes. For these applications where higher voltages/power density is needed, ionic liquids are useful since they have a larger electrochemical window compared to that of water-based electrolytes.

When ILs have been used in SC, the ILs have mostly been based on the imidazolium class of ILs, [7–10] but also others such as phosphonium-based ILs have been used to create SC. [24] Some of these are considered fairly safe and non-toxic, for example 1-ethyl-3-methylimidazolium ethyl sulfate (EcoEng) has been marketed as a greener alternative. But the most used and some of the best imidazolium SCs have been made using fluorinated anions, such as 1-ethyl-3-methylimidazolium bis(trifluoromethylsulfonyl)imide (EMIM:TFSI) or BF<sub>4</sub> and PF<sub>6</sub> salts. Organofluoride compounds are not a natural part of our ecosystem; they release toxic fumes when burned and should be avoided in widely spread devices, such as are targeted here.

We have instead investigated and used ionic liquids based on choline chloride (ChoCl). ChoCl is a quaternary ammonium salt and is widely used as chicken food additive to accelerate growth. We have used mixtures of ChoCl and urea, oxalic acid, ethylene glycol and sorbitol. Blending these create deep eutectic solvents that have similar properties to ILs [25,26]. These solvents are liquids or semi-liquids (syrup/gel) at room temperature. These ILs and EcoEng are here used to create environmentally friendly supercapacitors on paper. The IL EMIM:TFSI is used as a reference to compare the different ILs. To minimize the impact on the environment and create fully recyclable and/or biodegradable devices, the devices are printed on a paper substrate.

The electrodes used, in the laminated large supercapacitors presented in this paper, are printed using a rotary screen printer in a pilot scale production line. Several meters (~30 m) of electrodes were printed and stored on a 10 cm in diameter roll without delamination. The rest of the devices are fabricated on a laboratory scale using roll-to-roll (R2R) compatible technologies. So the final steps, including screen printing the IL, addition of the separator and lamination, could easily be scaled up to pilot scale production as well.

## 2. Experimental

The deep eutectic solvents (referred to as ILs in this paper) are created by mixing: ChoCl with different hydrogen bond donors. Mixtures with urea, oxalic acid and ethylene glycol were purchased from Scionix Ltd (Reline™, Oxaline™ and Glyceline™ respectively). For the sorbitol variant we mixed ChoCl with sorbitol (1:1 mol%) and heated it at 60 °C for 24 h to create the IL here called CSorb.

To characterize the devices two different supercapacitor structures were used in this paper; one type for measuring on a “standardized” SC and a second type with gold electrodes to clarify the role of the electrolyte/activated carbon interactions in the SC. In the first standardized SC structure the different ionic liquids are sandwiched between two reference activated carbon electrodes printed on PET film. The electrodes are separated using a rubber O-

ring, to ensure that consistent spacing is used in all measurements, creating a parallel plate capacitor. This is done so that the ILs can be compared to each other while keeping the electrodes and their configuration as similar as possible. The activated carbon electrodes combined with the different ILs are then characterized using electrical impedance spectroscopy. The ILs are also measured in a configuration using flat gold electrodes to more clearly see the IL effect. By comparing them to the standardized SC, one can more easily clarify the effect of using activated carbon containing a wide range of pore sizes. The devices made in the “commercial” approach, using R2R printed electrodes and R2R compatible device manufacturing, were characterized in the same manner. Here the PET substrate for the electrodes is replaced with aluminum coated paper (standard paper packing material) and a paper separator is used to minimize the distance between the electrodes without short circuiting the device. These devices were also bigger, having a capacitor area of  $56 \text{ cm}^2$ . The device was encapsulated by laminating it between two pieces of plastic using a standard office laminator. These supercapacitors were characterized with cyclic charge–discharge measurements (IEC 62391 standard) to see how good they would perform as a commercial device.

In the standardized SC structure, a  $100 \mu\text{m}$  thick PET laminated with a  $7 \mu\text{m}$  aluminum layer was used as substrate. As we are using polar ionic liquids which contain water and chlorides, and would inevitably oxidize (corrode) the aluminum electrodes within days, a layer of dense graphite ink (Acheson PF407A) is used to coat the aluminum to prevent this oxidation/corrosion. The ink was screen printed and cured at  $95^\circ\text{C}$ . To finalize the electrodes and supply the large area functionality, a  $70 \mu\text{m}$  thick layer of activated carbon (Norit DLC Super 30) is screen printed and dried at room temperature on top of the first carbon layer to create a layer that has a geometrical area of  $1 \text{ cm}^2$ . The AC was printed as a water-based ink that contained activated carbon and chitosan (ChitoClear fg90, Primex) binder in weight ratio 20:1. Approximately 60% water and 1.5% acetic acid was used as the solvent (the water amount was used to adjust the viscosity of the ink). Excluding the effect of the chitosan, the pure activated carbon, in this  $1 \times 1 \text{ cm}^2$  printed patch has a total surface area (B.E.T.) of  $1600 \text{ m}^2/\text{g}$  reported by the manufacturer. By using this value and the measured (by physical removal of the electrode) mass ( $5.62 \text{ mg cm}^{-2}$ ) of the AC electrodes (one half cell) the active area comes to roughly  $9.0 \text{ m}^2 \text{ cm}^{-2}$  of capacitor surface. The mass and thickness (measured using micrometer screw) ( $70 \mu\text{m}$ ) of the AC electrode was then used to calculate the electrode density. The density of pure graphite is  $2.23 \text{ g cm}^{-3}$  and was used to calculate the total volume of all voids in the AC electrode. It was calculated that 64% of the electrode was empty space. The theoretical amount of IL that would be absorbed into one capacitor is then  $2 \times 4.5 \mu\text{L cm}^{-2}$ . The AC electrodes are then submerged in the different ILs and left for at least 15 min in

order for the IL penetrate all the pores in the AC. A rubber O-ring is then used as a separator, in the measurement setup, to create a  $0.8 \text{ cm}^2$  capacitor with  $1.3 \text{ mm}$  separation between the electrodes.

In the commercial capacitor structure aluminum coated paper, Walki Pantenna Laminat, was used as the substrate. The paper was originally developed for use as substrate for RFID-antennas and the paper has a thin coat of plastic on both sides, one of which has an aluminum coat. The electrodes were printed on the aluminum side. The electrodes were printed on a pilot scale production line using a rotary screen printer running at  $2 \text{ m min}^{-1}$  and using screen mesh 64 (threads/inch). The same graphite ink and AC ink was used as described above. The electrodes were dried at  $140^\circ\text{C}$  for 2 min directly after each printing step using 4 ovens. The roll was then transferred to a new machine, where two further drying steps were performed to ensure full drying, maximal adhesion and maximal conductivity. The two final steps comprised of 12 s heating using a 5 kW IR lamp and 2 min using four  $140^\circ\text{C}$  ovens. The two first printing and heating steps were done at a speed of  $2 \text{ m min}^{-1}$  and the final two extra heating steps at  $1.5 \text{ m min}^{-1}$ .

The geometrical electrode area in the “commercial” printing trail was  $112 \text{ cm}^2$ , the graphite layer thickness  $18 \mu\text{m}$  and the AC thickness  $85 \mu\text{m}$ . The former was measured using a Veeco Wyko NT3300 white-light interferometer and the latter using a micrometer screw. The measured mass of the AC in these electrodes (one half cell) is  $3.91 \text{ mg cm}^{-2}$ . The different ILs were then screen printed on top of/into the AC electrodes, using two passes on a flatbed screen printer (screen mesh 25) to ensure pore filling (the filling occurred during the printing process, as seen by the naked eye). Using the same method as described above, the active electrode area of one half cell comes to  $6.3 \text{ m}^2 \text{ cm}^{-2}$  and the total volume of empty space 79% of the total electrode volume. According to this  $2 \times 6.7 \mu\text{L cm}^{-2}$  will be absorbed into the AC electrode. As these AC electrodes are less dense than the ones used in the standardized SC (due to differences in processing), the internal resistance will likely be larger as the individual carbon grains are further apart. On the other hand, it might be that as the grains are less densely packed, a larger surface area might be available for the electric double layers to form.

In order to save material the electrodes produced ( $112 \text{ cm}^2$ ) were cut in half and the area used for each supercapacitor was  $56 \text{ cm}^2$ . A NKK TF40-50 cellulose paper was used as a separator in these devices. The thickness of the paper is about  $50 \mu\text{m}$  (this separator absorbs some of the extra IL used). In order to achieve a practical component, the supercapacitors were then laminated using standard office heat lamination equipment, creating a roughly  $0.6\text{--}0.7 \text{ mm}$  thick encapsulated package. The structure of the commercial approach can be seen in Fig. 1. The impedance spectroscopy was performed by running in tripolar potentiostatic mode using a Gamry 600 Impedance Spectrometer. The confocal

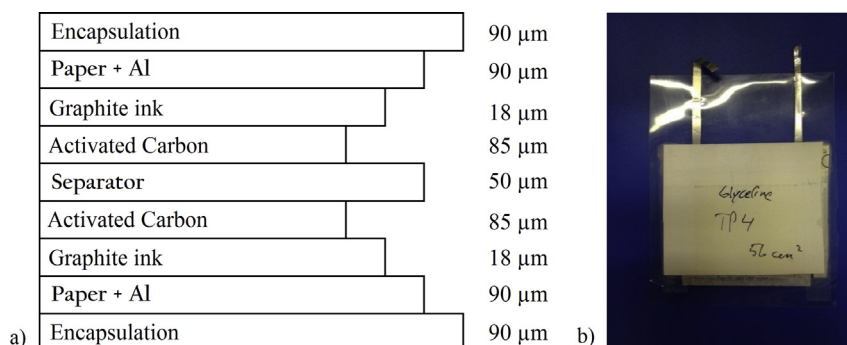
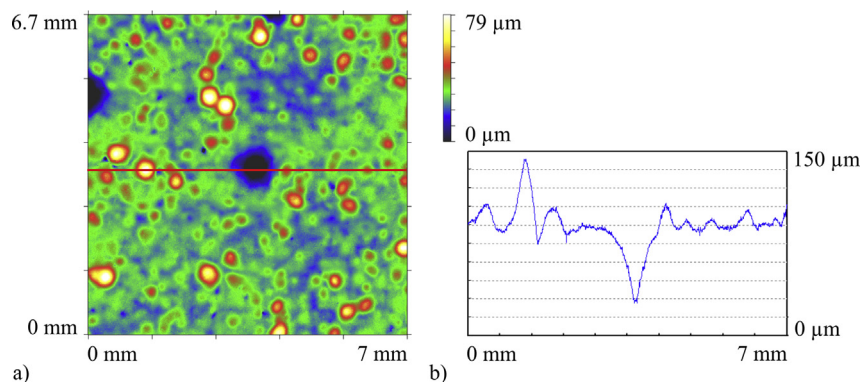


Fig. 1. (a) Internal structure and thicknesses of the laminated supercapacitors and (b) a photograph of a laminated  $56 \text{ cm}^2$  commercial SC fabricated on paper.



**Fig. 2.** (a) A stitched 7 mm × 6.7 mm confocal image of the AC surface and a profile of the red line is plotted in (b). (For interpretation of the references to color in this figure legend, the reader is referred to the web version of this article.)

optical white-light microscopy image was recorded with a Nano-focus  $\mu$ Surf microscope. A 10× (primary image size 1.6 × 1.54 mm) magnifying lens was used, and the image recorded is a 5 × 5 stitch, giving a total image size of 7 × 6.7 mm.

### 3. Results and discussion

A confocal microscopy image including a profile of the printed activated carbon electrodes can be seen in Fig. 2. There is a pattern of hills and valleys with regular intervals in the film. This is a result of the screen mesh used in printing of the AC electrode. Some pinholes, down to the underlying carbon layer, can also be seen that are around 80  $\mu$ m deep corresponding to the film thickness. Some peaks on the same length scale, probably caused by clogging and subsequent release of extra material in the next printing pass, can also be seen. As such, neither of them have any significant effect on the supercapacitor performance.

In the impedance spectroscopy measurements the frequency was scanned from 1 MHz to 100 mHz. The capacitance,  $C$ , was calculated using  $C = 1/(-Z_{\text{Im}}2\pi fA)$ , where  $Z_{\text{Im}}$  is the imaginary part of the impedance,  $f$  is the frequency and  $A$  is the area of the capacitor [27]. The conductivity,  $\sigma$ , was calculated using  $\sigma = d/(AZ_{\text{Re}})$ , where  $d$  is the separation and  $Z_{\text{Re}}$  is the real part of the impedance [27]. The Nyquist plot seen in Fig. 3 is plotted in log–log scale to better show the large difference observed for the different

ILs. The ionic liquid EMIM:TFSI is used as a reference to compare the environmentally friendly ILs to. It is clear that the internal resistances of the environmentally friendly ILs are larger than that of the reference. This is mainly due to differences in viscosity and hence ion mobility. Of the alternative ionic liquids EcoEng has the lowest and CSorb largest internal resistance. Viscosity plays a large role here as CSorb clearly is the most viscous at room temperature (thick paste) followed by Reline and so on, mapping the internal resistance values. From the capacitance graph in Fig. 4 it can be seen that the same trend is present here where the capacitance curve for CSorb is shifted towards lower frequencies compared to the others. The conductivity curves in Fig. 4 are also in agreement with this conclusion. A measurement was done for a Reline SC (high viscosity), to test this conclusion, where the real part of the impedance ( $\propto$  internal resistance) at 100 kHz was plotted as a function of the IL temperature (not shown). The impedance was measured to be 4.4  $\Omega$  at 93.5  $^{\circ}\text{C}$  and 243  $\Omega$  at 24  $^{\circ}\text{C}$  confirming the conclusion above. However, for low-power applications of a supercapacitor a large internal resistance might not be an obstacle.

As the AC contains several different ranges of pore sizes, the size of the IL molecule and stacking as well as wetting of the pores can be crucial for the performance of the capacitor [28]. An IL that forms large hydrogen bonded matrices might not reach the smaller pores resulting in lower capacitances or if the wetting behavior is not optimal erroneous values will be measured (i.e. more a SC device issue than an IL issue). To investigate if that is the case and find more “true” characteristics for the ILs, smooth evaporated gold electrodes were used to create parallel plate capacitors using the environmentally friendly ILs as electrolyte, and again comparing them to the EMIM:TFSI standard. The phase angle of the impedance measurements was used to determine at which frequencies the capacitor turns capacitive. When the phase angle is around  $-90^{\circ}$  it is capacitive and more resistive at lower angles. It can be seen from Fig. 5 (smooth electrodes) that EcoEng (and EMIM:TFSI) is capacitive at much higher frequencies compared to the others whereas in Fig. 4 (porous electrodes) the capacitance curve of EcoEng follows the same line as the other (better) ones. This apparent inconsistency between the smooth- and the porous-electrode-SCs could be explained by different wetting properties where the motion of EcoEng into the pores might be more obstructed than for the other ILs. According to these experiments none of the ILs can definitely be excluded as candidates for use in environmentally friendly supercapacitors.

The “commercial” supercapacitors manufactured on paper were characterized using cyclic charge–discharge in constant current discharge mode according to the IEC 62391 standard. [29] An example of such a cycle applied on a SC can be seen in Fig. 6. The

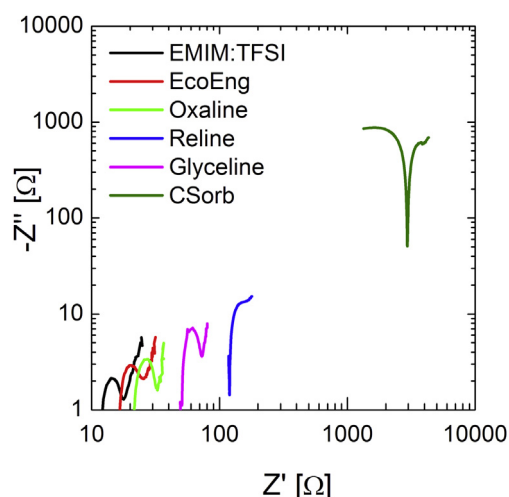


**Fig. 3.** Nyquist plot of the 0.8 cm<sup>2</sup> standardized SC fabricated using different ILs. The axes are plotted on logarithmic scales due to the large differences in the impedances.



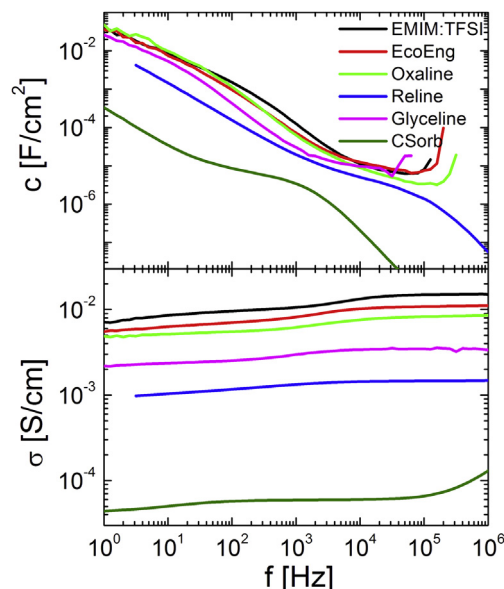


Fig. 4. The capacitance, above, and conductivity, below, of the 0.8 cm<sup>2</sup> standardized SC fabricated on PET.

minimum and maximum voltage applied in these measurements is 0.2 V and 1.5 V, respectively. Depending on the speed at which the capacitors could be charged, the current applied ranged between 2 mA and 20 mA. The capacitor is first charged and discharged three times at constant current. This is done to ensure that all the capacitors have had the same history and also that all the pores in the AC electrodes are filled. During the next step (30 min) the amount of current needed to keep the capacitor charged at maximum voltage is measured. This is done to make sure the capacitor is properly charged before the capacitor is discharged at a constant current. During this discharge step the characteristic electrical values for the capacitor are defined. They include the capacitance,  $C = I(t_2 - t_1)/(V_2 - V_1)$ , where  $I$  is the discharge current and  $t_1$ ,  $t_2$ ,  $V_1$  and  $V_2$  are the times and voltages that describe the slope of the voltage drop during the step, the internal resistance,  $R_i = \Delta V/I$ , where  $\Delta V$  is the voltage difference between the maximum voltage,  $V_{MAX}$ , and the voltage at the intersection of the above mentioned slope and the time at the start of this step. The maximum energy stored in the device,  $W_{MAX}$ , for a capacitor,  $C$ , with the internal

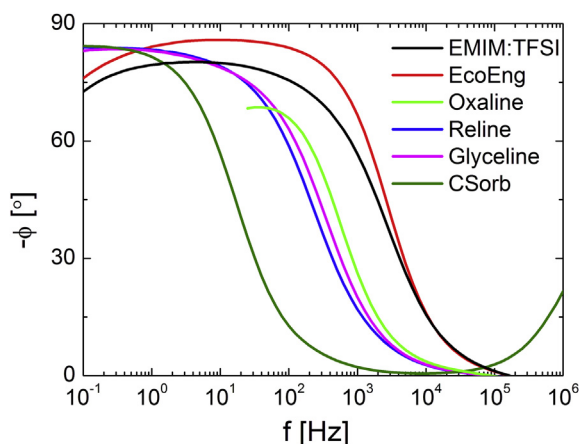


Fig. 5. Phase angle of the ILs sandwiched between 0.5 cm<sup>2</sup> Au electrodes evaporated on glass. The electrodes were separated by 100 μm.

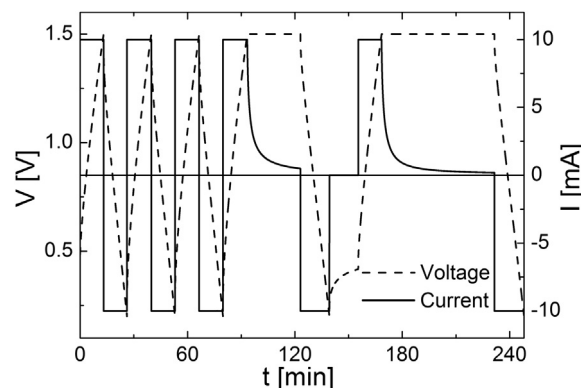


Fig. 6. Example output of one cyclic charge–discharge measurement.

resistance (connected in series),  $R_i$ , connected in parallel to an external load,  $R_L$ , is calculated using  $W_{MAX} = \frac{1}{2}CV_{MAX}^2$ . [1]  $V_{MAX} = 1.5$  V has been used for all devices since this was the value used in the CCD measurements. A common voltage was chosen for all the different SCs so that they could be compared to each other and simultaneously keep the leakage current low. The actual maximum voltage for all the different electrolytes is also difficult to determine since there is no sharp increase in the cyclic voltammetry measurements (not shown). Using a higher voltage would directly improve the device characteristics. The energy available at the load,  $W_L$ , can then be calculated using:

$$W_L = R_L W_{MAX} / (R_L + R_i) \quad (1)$$

and the power available at the load,  $P_L$ :

$$P_L = V_{MAX}^2 R_L / (R_L + R_i)^2 \quad (2)$$

The maximum available power at the load,  $P_{MAX}$ , is then found in the special, impedance matching, case when  $R_L = R_i$ . After the discharge the capacitor is charged to  $V_{MAX}$  and kept there for an hour. The leakage current,  $I_{LEAK}$ , is then defined as the current at the end of this 60 min step. Finally the capacitor is discharged to  $V_{MIN} = 0.2$  V. The maximum voltage used is 1.5 V. The different values obtained for each IL is shown in Table 1. The values reported correspond to a one square centimeter capacitor. The values have been calculated as if the capacitor was constructed of 56 capacitors connected in parallel. CSorb has the lowest capacitance and highest internal resistance. This is mainly due to its high viscosity at room temperature resulting in poor ion conductivity and wetting properties. Even though EcoEng has slightly higher internal resistance than e.g. EMIM:TFSI the capacitance is still very high. Overall, Glyceline out-performs the other ILs including EMIM-TFSI and EcoEng. It has the highest capacitance and lowest internal resistance. Comparing the internal resistances of the different electrolytes in the standardized versus the commercial SC structure it can be seen that Glyceline and EcoEng are in reverse order in the two structures. The reason for this might be different wetting properties

Table 1  
Summary of the electrical characteristics of the 56 cm<sup>2</sup> commercial SC fabricated on paper.

Ionic liquid	C [mF cm <sup>-2</sup> ]	$R_i$ [kΩ cm <sup>-2</sup> ]	$W_{MAX}$ [μWh cm <sup>-2</sup> ]	$P_{MAX}$ [μW cm <sup>-2</sup> ]	$I_{LEAK}$ [μA cm <sup>-2</sup> ]
EcoEng	173	1	54	554	7
EMIM:TFSI	148	0.7	46	793	3
Glyceline	173	0.3	54	1614	11
Oxaline	127	2	40	244	61
CSorb	44	13	14	45	9

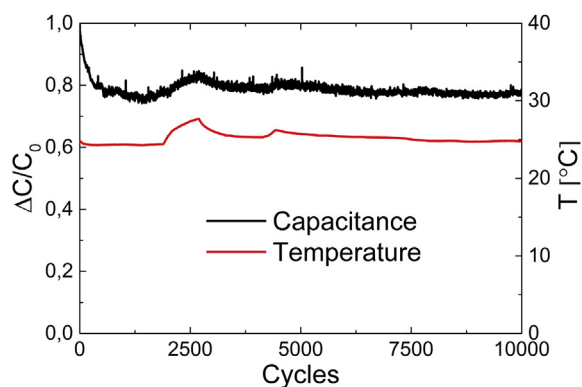


**Fig. 7.** Cyclic charge and discharge measurement of a 1 cm<sup>2</sup> Glyceline SC. The black curve represents the capacitance for each cycle and the red curve the temperature. (For interpretation of the references to color in this figure legend, the reader is referred to the web version of this article.)

for the materials in the two different structures when using the chosen commercial fabrication processes. Glyceline also has the highest internal energy and power density. This is surprising as it does not have the highest conductivity nor so different structure compared to the other Choline-chloride based ILs. One explanation could be that the relative small ion size of chloride (compared to for example TFSI) in the case of Glyceline plays a role; as it might not be as “solvated” (or clustered) in ethylene glycol as in the other cases and hence more easily get attracted to the AC surface, and hence pack more densely. Another, perhaps more likely explanation is that the differences in wetting and pore penetration might be very different for the different ILs, and if for example Glyceline is good at wetting all surfaces, the active surface area accessible will be higher.

To clarify the cycling stability of these environmentally friendly SCs smaller 1 cm<sup>2</sup> Glyceline SC were fabricated and laminated on PET. The small size was chosen in order to increase the speed at which the device could be charged and discharged. In order to minimize the possible effect of water the SC was charged between 0.2 V and 1.2 V at  $\pm 0.003$  A for a total of 10,000 cycles. The capacitance was calculated and normalized for each individual cycle and the results are plotted in Fig. 7. The temperature of the measuring atmosphere has also been included in the graph. It can be seen that an initial decrease in capacitance is present. This is most likely due to the shape of the laminated capacitor reaching a stable form (trapped air moving around). After that the capacitance remains effectively unchanged for the remainder of the 10,000 cycle measurement. The small variations observed perfectly follow the change in the room temperature.

The operating window of these supercapacitors can be increased directly by increasing the voltage ( $V_{MAX}$ ) used, cyclic voltammetry measurements performed up to 2.5 V confirm this (not shown), or by connecting several layers in parallel. The  $V_{MAX}$  will be different depending on the IL and water content, so further studies will be needed. In this study, however, only the feasibility of using these ILs as electrolyte in printed supercapacitors was

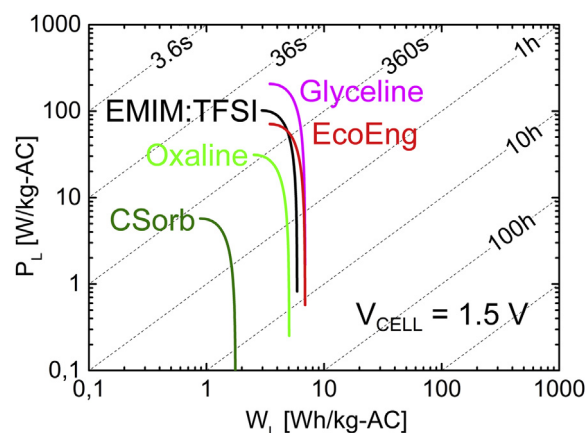


**Fig. 8.** A Ragone plot of the different 56 cm<sup>2</sup> commercial supercapacitors.

investigated and further studies on electrochemical window, influence of water content and possible balancing issues when series connecting will be needed. To give more comparable values, in Table 2 the same characteristic values (reported in Table 1) have been reported per kilogram of activated carbon used in the SCs. Also, by using Equations (1) and (2) the available power density and available energy density for an external load connected to the different IL SCs have been plotted in a Ragone chart. The values have been scaled by the mass of the AC used in the devices and plotted for different external loads ranging from  $R_L = R_i$  to  $R_L \approx 500R_i$ . From Fig. 8 it can be seen that the Glyceline SC has the highest power compared to the other IL SCs, including the reference IL SCs. In order to better understand how these SCs perform a comparison with commercially available SCs is made. A few approximations are done in the following discussion, in order for the comparison to be useful. This is due to the fact that our devices are done on a laboratory scale and are measured at lower voltages than the commercially available ones. Energy- and power density values for commercial SCs with organic electrolytes have been reported by A. Burke. [30] Compared to those, our SC energy density is on the same level. Our maximum energy density (for the Glyceline SC) is about 7 Wh kg<sup>-1</sup> when calculated using 1.5 V potential. The value should be multiplied by  $2.7^2/1.5^2$  if the potential was 2.7 V instead of 1.5 V, resulting in an energy density of 22 Wh kg<sup>-1</sup>. If 25% of the mass (as is typical for the SCs listed in Ref. [30]) of the complete SC is AC, this would correspond to about 5 Wh kg<sup>-1</sup> in a complete SC component. Typical values for e.g. Maxwell's and Nesscap's SCs are also about 5 Wh kg<sup>-1</sup>. On the other hand, our power densities are clearly lower compared to the commercially available ones. Again, to make a valid comparison, our values should be modified in order to compensate for the potential- and structural difference. The same commercial Maxwell and Nesscap SCs have matched impedance power densities around 8–10 kW kg<sup>-1</sup>. This is on the order of 50 times higher than the power densities in our devices. This is partially due to the non-optimized SC geometry, but the main reason is the relatively low conductivity of our ionic liquid electrolytes. Together these two factors increase the equivalent series resistance, resulting in lower power densities. As a cheap and “green” alternative, and in applications where high power is not necessarily required, these environmentally friendly SCs can be a viable alternative.

#### 4. Conclusions

Non-Faradaic supercapacitors made with printing techniques, using symmetrical activated carbon electrodes and environmentally

**Table 2**

Electrical values for the 56 cm<sup>2</sup> commercial SC on paper given per kilogram of AC carbon used in the capacitor.

Ionic liquid	C [kF kg <sup>-1</sup> ]	$W_{MAX}$ [Wh kg <sup>-1</sup> ]	$P_{MAX}$ [W kg <sup>-1</sup> ]
EcoEng	22	7	71
EMIM:TFSI	19	6	101
Glyceline	22	7	206
Oxaline	16	5	31
CSorb	6	2	6

friendly ionic liquids as electrolyte were investigated as an environmentally friendly power source. The whole device is printed with existing printing and lamination equipment onto commercial materials, including the electrodes which were printed using a pilot scale printer. The approach can easily be up scaled to pilot scale and even industrial scale with minor effort. As the device is environmentally friendly; with commercial grade of a paper substrate, activated carbon electrodes and ionic liquids based on choline chloride, and the materials and fabrication processes are inexpensive – we propose these SCs to be used both in large and small size applications that require burnable and/or recyclable materials. Cyclic charge–discharge measurements and impedance spectroscopy measurements on the different ionic liquids showed that Glyceline™ not only outperformed the other environmentally friendly ionic liquids including EcoEng™, but also reference ionic liquid EMIM:TFSI. Further work on why Glyceline™ was especially good and cost analyzes when scaling up this approach is needed, before a commercial viable product can be reached. The performances of these SCs are, however, excellent for this purpose.

### Acknowledgments

This work was done within the Tekes funded PRISU project. The authors would like to acknowledge Max Johansson for the confocal microscopy images and valuable discussions.

### References

- [1] B.E. Conway, *Electrochemical Supercapacitors: Scientific Fundamentals and Technological Applications*, Kluwer Academic/Plenum Press, New York, 1999.
- [2] M. Toupin, D. Bélanger, I.R. Hill, D. Quinn, *J. Power Sources* 140 (2005) 203.
- [3] S. Mitali, D. Soma, D. Monica, *Res. J. Chem. Sci.* 1 (2011) 109.
- [4] M. Ue, K. Ida, S. Mori, *J. Electrochem. Soc.* 141 (1994) 2989.
- [5] P. Kurzweil, M. Chwistek, *J. Power Sources* 176 (2008) 555.
- [6] R. Kötz, M. Hahn, R. Gallay, *J. Power Sources* 154 (2006) 550.
- [7] G. Wang, L. Zhang, J. Zhang, *Chem. Soc. Rev.* 41 (2012) 797.
- [8] A. Burke, *Electrochim. Acta* 53 (2007) 1083.
- [9] P.J. Hall, M. Mirzaeian, S.I. Fletcher, F.B. Sillars, A.J.R. Rennie, G.O. Shitta-Bey, G. Wilson, A. Cruden, R. Carter, *Energy Environ. Sci.* 3 (2010) 1238.
- [10] Y. Zhu, S. Murali, M.D. Stoller, K.J. Ganesh, W. Cai, P.J. Ferreira, A. Pirkle, R.M. Wallace, K.A. Cychosz, M. Thommes, D. Su, E.A. Stach, R.S. Ruoff, *Science* 332 (2011) 1537.
- [11] R. Moscatiello, *SGIA J.* 9 (2005).
- [12] J. Keskinen, E. Sivonen, M. Bergelin, J.E. Eriksson, P. Sjöberg-Eerola, M. Valkiainen, M. Smolander, A. Vaari, J. Uotila, H. Boer, S. Tuurala, *Adv. Sci. Technol.* 72 (2010) 331.
- [13] O.S. Nissen, H.C. Beck, M. Schou, *Double Layer Capacitor and Its Manufacturing Method*, US6341057, 2002.
- [14] J. Lang, *Electrochemical Capacitor and Method for Its Preparation*, US 2005/0007727, 2004.
- [15] L. Wei, G. Yushin, *Nano Energy* (2012).
- [16] M. Kaempgen, C.K. Chan, J. Ma, Y. Cui, G. Gruner, *Nano Lett.* 9 (2009) 1872.
- [17] J. Keskinen, E. Sivonen, S. Jussila, M. Bergelin, M. Johansson, A. Vaari, M. Smolander, *Electrochim. Acta* 85 (2012) 302.
- [18] K. Jost, C.R. Perez, J.K. McDonough, V. Presser, M. Heon, G. Dion, Y. Gogotsi, *Energy Environ. Sci.* 4 (2011) 5060.
- [19] L. Hu, H. Wu, Y. Cui, *Appl. Phys. Lett.* 96 (2010) 183502.
- [20] L.T. Le, M.H. Ervin, H. Qiu, B.E. Fuchs, W.Y. Lee, *Electrochem. Commun.* 13 (2011) 355.
- [21] P. Kossyrev, *J. Power Sources* 201 (2012) 347.
- [22] C. Meng, C. Liu, L. Chen, C. Hu, S. Fan, *Nano Lett.* 10 (2010) 4025.
- [23] V.L. Pushparaj, M.M. Shaijumon, A. Kumar, S. Murugesan, L. Ci, R. Vajtai, R.J. Linhardt, O. Nalamasu, P.M. Ajayan, *Proc. Natl. Acad. Sci. U. S. A.* 104 (2007) 13574.
- [24] K.J. Fraser, D.R. MacFarlane, *Aust. J. Chem.* 62 (2009) 309.
- [25] A.P. Abbott, D. Boothby, G. Capper, D.L. Davies, R.K. Rasheed, *J. Am. Chem. Soc.* 126 (2004) 9142.
- [26] A.P. Abbott, G. Capper, D.L. Davies, R.K. Rasheed, V. Tambyrajah, *Chem. Commun.* (2003) 70.
- [27] C.-S. Lim, K.H. Teoh, C.-W. Liew, S. Ramesh, *Mater. Chem. Phys.* 143 (2014) 661.
- [28] P. Simon, Y. Gogotsi, *Nat. Mater.* 7 (2008) 845.
- [29] Standard IEC 62391, *Fixed Electric Double-layer Capacitors for Use in Electronic Equipment*, 2006.
- [30] A. Burke, in: *Ultracapacitors in Place of Batteries in Micro- and Mild Hybrid Vehicles, Supercapacitors Europe 2014*, IdTechEx, 1–2 April 2014.